

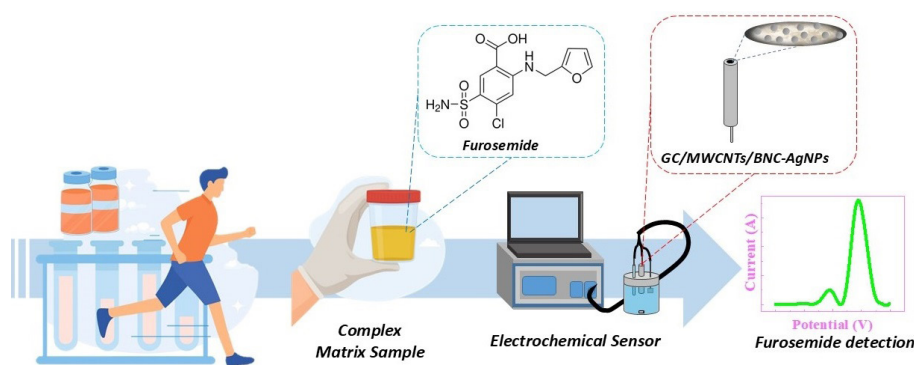


ARTICLE

# Sustainable Engineering of a Surfactant-Free Nanocomposite Based on Bacterial Nanocellulose Produced from Beer Waste and MWCNTs-AgNPs for Electrochemical Sensing of Furosemide

Gloria Tersis Vieira dos Santos , Francisco Contini Barreto , Martin Kássio Leme da Silva , Ivana Cesarino\*  

Universidade Estadual Paulista (Unesp) , Departamento de Bioprocessos e Biotecnologia, Botucatu, SP, 18610-034, Brazil



Graphical abstract created with the assistance of ChatGPT and Gemini; final version by the authors.

Carbon-based nanomaterials, particularly multi-walled carbon nanotubes (MWCNTs), are widely used in electrochemical sensors due to their high conductivity and large surface area. However, their poor dispersion often requires synthetic surfactants. Biopolymers such as cellulose have emerged as promising sustainable dispersing agents. In this context, bacterial nanocellulose (BNC) produced from waste offers a green alternative with potential to stabilize and disperse MWCNTs in aqueous media. Herein, a surfactant-free nanocomposite based on BNC produced from beer waste and MWCNTs modified with silver nanoparticles (AgNPs) was engineered to modify electrochemical sensors for pharmaceutical detection of furosemide. The morphology, composition, and electrochemical properties of the nanocomposite were characterized by scanning electron microscopy (SEM) with energy-dispersive X-ray spectroscopy (EDS), cyclic voltammetry (CV), electrochemical impedance spectroscopy (EIS), and differential pulse voltammetry (DPV). Furosemide oxidation was evaluated in aqueous medium and synthetic urine using a glassy carbon electrode modified with the MWCNTs/BNC-AgNPs film, and voltammetric parameters were optimized to enhance the analytical response. The sensor presented a linear range from 5.0 to 65.0  $\mu\text{mol L}^{-1}$ , with limits of detection and quantification of 0.19 and 0.64  $\mu\text{mol L}^{-1}$ , respectively. These findings demonstrate the high sensitivity and practical applicability of the MWCNTs/BNC-AgNPs-modified electrode for reliable furosemide determination in urine samples.

**Cite:** dos Santos, G. T. V.; Barreto, F. C.; da Silva, M. K. L.; Cesarino, I. Sustainable Engineering of a Surfactant-Free Nanocomposite Based on Bacterial Nanocellulose Produced from Beer Waste and MWCNTs-AgNPs for Electrochemical Sensing of Furosemide. *Braz. J. Anal. Chem.* (Forthcoming). <https://doi.org/10.30744/brjac.2179-3425.AR-117-2025>

**Received:** December 14, 2025; **Revised:** March 17, 2026; **Accepted:** April 8, 2026; **Published online:** April 2026.

This article was submitted to the BrJAC Special Issue dedicated to Prof. Dr. Lauro Tatsuo Kubota.

**Keywords:** nanomaterials, cellulose, multi-walled carbon nanotubes, electrochemical sensors, pharmaceuticals

## INTRODUCTION

Carbon nanomaterials (CNMs) are widely used in electrochemical sensors due to their excellent electrical conductivity, large surface area and chemical stability, desirable characteristics to a high sensitivity and selective sensor, such as carbon nanotubes (CNTs).<sup>1</sup> Over the past decade, considerable efforts have focused on embedding CNTs within polymer matrices to generate innovative CNMs that combine high conductivity with multifunctional properties.<sup>1</sup> However, CNTs tend to form agglomerates, leading to their poor dispersion into the polymer matrix, reducing mechanical and electrical properties of the composite.<sup>2,3</sup>

Various chemical and physical approaches have been employed to facilitate CNTs dispersion and enhance their solubility in both aqueous and non-aqueous media.<sup>4,5</sup> Covalent functionalization with strong acids can promote CNTs dispersion by introducing defects on their sidewalls, but this damage can compromise their mechanical, electrical, and thermal properties. Surfactants such as sodium dodecyl sulfate (SDS) have also been applied to disperse CNTs,<sup>1,4</sup> but they often require additional purification steps because residual molecules can remain adsorbed, thereby altering CNTs properties.<sup>6</sup> As an alternative, nanocellulose has been investigated, as it can improve ionic conductivity in sensing applications<sup>5</sup> and provide greater stability.<sup>4</sup>

Nanocellulose (NC) is a biodegradable and natural biopolymer that has shown great potential as an environmentally friendly dispersing agent for CNTs.<sup>7,8</sup> Current strategies for preparing CNTs/NC composites often involve polluting chemicals or multi-step synthesis routes, which limit their scalability and environmental viability.<sup>9</sup> Moreover, the interaction between NC and CNTs strongly depends on the nanocellulose type, directly influencing the electrochemical performance of composites.<sup>5</sup> Improving the effective interaction between NC and CNTs, while simplifying synthesis and minimizing harmful residues, remains an essential challenge for obtaining composites with optimized architecture, mechanical strength, conductivity, and stability.<sup>10</sup>

Bacterial nanocellulose (BNC) can be produced using agricultural waste as a substrate for bacterial fermentation, which reduces production costs and contributes to more sustainable processes.<sup>11</sup> BNC presents a highly porous nanofibrillar network with a large surface area, providing numerous anchoring sites for conductive materials and nanoparticles.<sup>12</sup> Due to these characteristics, BNC-based nanocomposites exhibit favorable properties such as biocompatibility, structural stability, and improved interaction with electroactive materials.<sup>13,14</sup> These conductive nanocomposites have been widely explored in the development of electrochemical sensors and electrodes, including the modification of glassy carbon (GC) electrodes to enhance electrochemical performance for the detection of analytes such as pharmaceutical compounds.<sup>15</sup>

Furosemide (FUR) is a diuretic commonly prescribed for the treatment of renal and cardiovascular disorders.<sup>16</sup> Monitoring its dosage during therapy is essential since it is a potent drug that has also been misused by athletes to mask the intake of illicit substances.<sup>17</sup> Conventional methods such as electrophoresis, spectrometry, and chromatography are widely employed for FUR quantification, but they present limitations due to their high cost, long analysis time, and need for complex sample pretreatment.<sup>17-19</sup> Electrochemical sensors, on the other hand, provide rapid response, high sensitivity, and simple operation.<sup>18</sup>

Therefore, the aim of this work is to engineer a nanocomposite based on carbon nanotubes, bacterial nanocellulose produced from beer waste, and silver nanoparticles, synthesized in water through a simple and surfactant-free process, modifying a glassy carbon electrode for electrochemical detection of furosemide.

## MATERIALS AND METHODS

### *Instrumentation*

Electrochemical analyses were conducted through NOVA 2.1 software, using a conventional three-electrode setup connected to PGSTAT128N potentiostat (Autolab Electrochemical System, Utrecht, The Netherlands). An Ag/AgCl (3.0 mol L<sup>-1</sup> KCl) electrode performed as the reference, a platinum plate served as the counter electrode, and a glassy carbon electrode (GC) was employed as the working electrode. Three configurations for GC were evaluated, including unmodified, modified with multi-walled carbon nanotubes and silver nanoparticles (GC/MWCNTs-AgNPs) and modified with multi-walled carbon nanotubes, bacterial nanocellulose and silver nanoparticles (GC/MWCNTs/BNC-AgNPs).

The composites were characterized at the Advanced Microscopy Laboratory of the Institute of Chemistry, São Paulo State University (LMA-IQ-Unesp) in Araraquara, SP, Brazil, using a high-resolution scanning electron microscope (FEG-SEM, JEOL JSM-IT500HR), equipped with secondary electron (SE) and backscattered electron (BSE) detectors, as well as an X-ray energy dispersive spectroscopy (XEDS) system. ImageJ software was used to measure the nanoparticle size.

### **Chemicals and solutions**

To prepare all solutions, ultrapure water (resistivity  $\geq 18 \text{ M}\Omega \text{ cm}$ ) obtained from a PURELAB Q, ELGA-VEOLIA was utilized. The reagents used in this study were: multi-walled carbon nanotubes (MWCNTs) (O.D.  $\times$  L = 6–9 nm  $\times$  5  $\mu\text{m}$ ) ( $\geq 98\%$ ), silver nitrate ( $\text{AgNO}_3$ ) ( $\geq 99\%$ ), ethanol, sodium borohydride ( $\text{NaBH}_4$ ), potassium phosphate monobasic ( $\text{KH}_2\text{PO}_4$ ), sodium phosphate dibasic ( $\text{Na}_2\text{HPO}_4$ ), calcium chloride dihydrate ( $\text{CaCl}_2$ ) ( $\geq 99.0\%$ ), sodium chloride ( $\text{NaCl}$ ) ( $\geq 99.0\%$ ), sodium sulfate ( $\text{Na}_2\text{SO}_4$ ) ( $\geq 99.0\%$ ), potassium chloride ( $\text{KCl}$ ) ( $\geq 99.0\%$ ), ammonium chloride ( $\text{NH}_4\text{Cl}$ ) ( $\geq 99.99\%$ ), urea ( $\geq 99.0\%$ ), alumina (0.3  $\mu\text{m}$ ), furosemide and estriol standard for AAS, nitric acid ( $\text{HNO}_3$ ) ( $\geq 90\%$ ), sulfuric acid ( $\text{H}_2\text{SO}_4$ ) ( $\geq 95\%$ ), copper standard solution (1000  $\text{mg L}^{-1}$  in  $\text{HNO}_3$ ), all reagents from Sigma-Aldrich (São Paulo, Brazil).

Bacterial nanocellulose was produced at Residual – Laboratory of Solid Waste and Composites (Unesp, Botucatu, SP, Brazil), with citric acid  $\text{C}_6\text{H}_8\text{O}_7$  from Êxodo Científica (Brazil), dipotassium phosphate ( $\text{K}_2\text{HPO}_4$ ), ammonium sulfate ( $(\text{NH}_4)_2\text{SO}_4$ ) and magnesium sulfate ( $\text{MgSO}_4$ ) from Synth (Brazil). A 4% NaOH solution was prepared with NaOH and distilled water. The sucrose ( $\text{C}_{12}\text{H}_{22}\text{O}_{11}$ ) required for the culture medium was replaced by market crystal sugar.

A 3:1 mixture of  $\text{H}_2\text{SO}_4/\text{HNO}_3$  (500 mL) was used to functionalize 1.0 g of MWCNTs for 14 h under constant stirring. The suspension was then filtered through a 0.45  $\mu\text{m}$  GVS nylon membrane. The material retained on the membrane was thoroughly washed with ultrapure water until neutral pH was achieved and subsequently dried in an oven at 60  $^\circ\text{C}$ .

### **Bacterial nanocellulose from waste synthesis**

The culture medium composition was adopted as reported by Borro et al.,<sup>20</sup> containing 100  $\text{g L}^{-1}$  sucrose, 6  $\text{g L}^{-1}$  citric acid, 5  $\text{g L}^{-1}$  yeast waste from brewing, 5  $\text{g L}^{-1}$  of phosphate potassium, 0.6  $\text{g L}^{-1}$  ammonium sulfate, and 0.2  $\text{g L}^{-1}$  magnesium sulfate. The medium pH was adjusted to 4.8 using 4% NaOH. The culture medium was autoclaved at 121  $^\circ\text{C}$  and 110 kPa for 15 min and then allowed to cool to room temperature. The strain *Gluconacetobacter xylinus* was inoculated, and incubations were performed at 28  $^\circ\text{C}$  under static conditions for 7 days. After incubation, the BNC was rinsed with distilled water to remove residual medium and then treated with 4% NaOH at 70  $^\circ\text{C}$  for 30 min to inactivate the bacterial cells. The BNC was subsequently washed with distilled water at room temperature until completely purified and colorless. The BNC was subsequently lyophilized, milled, and sieved to produce a fine powder for subsequent use in the synthesis of the nanocomposite, as shown in Figure 1 (section 1).

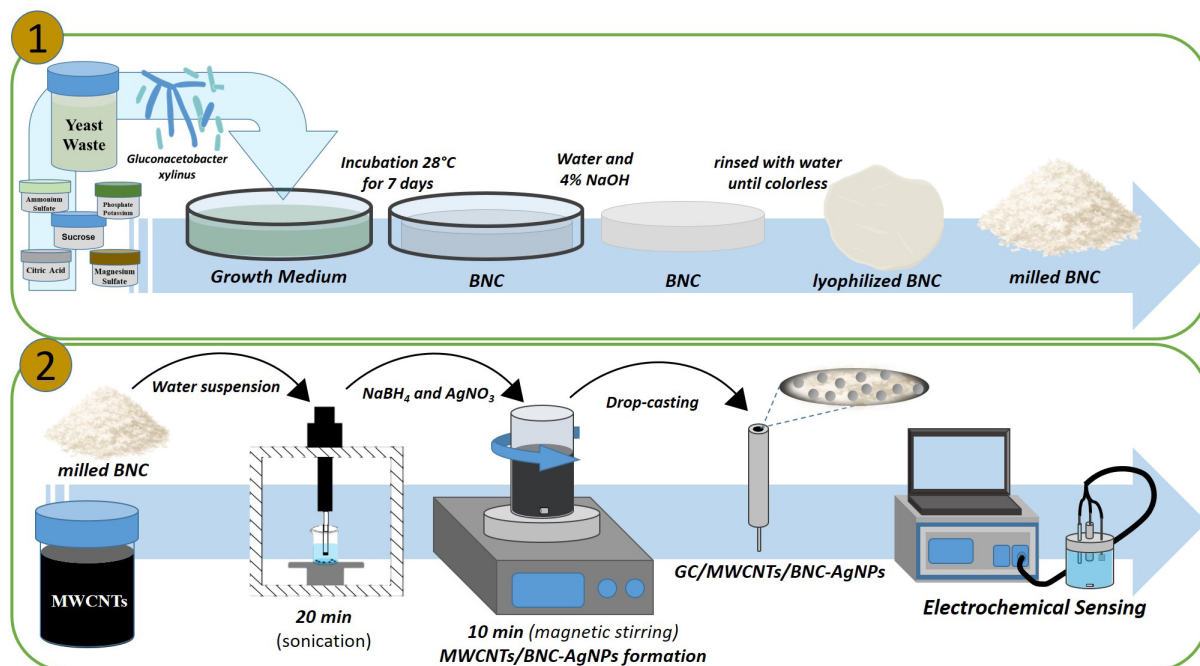


**Figure 1.** Overview of the workflow used to obtain the MWCNTs/BNC-AgNPs sensor. Step 1: *Gluconacetobacter xylinus* grows on a yeast-waste medium to form BNC, which is purified, lyophilized, and milled. Step 2: The milled BNC is dispersed with MWCNTs, reduced with NaBH<sub>4</sub>/AgNO<sub>3</sub> to form BNC-AgNPs, and the resulting nanocomposite is drop-cast onto a GC electrode for electrochemical detection of furosemide. [This figure was created with the assistance of ChatGPT and Gemini. The final design and content were developed and approved by the authors.]

### Nanocomposite synthesis

The composite was synthesized in a beaker containing 2.0 mg of BNC in 20 mL of ultrapure water and sonicated using a QSonica sonicator for 20 min at 75% amplitude. Subsequently, 20 mg of functionalized MWCNTs were added, and the mixture was sonicated again for 10 min.

For the incorporation of silver nanoparticles, 13 mg of sodium borohydride (NaBH<sub>4</sub>) was first added to the solution as a reducing agent for the silver nitrate to be added subsequently, and the mixture was processed in an ultrasonic bath (power = 210 W and frequency = 40 kHz) for 30 min. Then, 8 mg of silver nitrate (AgNO<sub>3</sub>) was dissolved in 2 mL of ethanol and added dropwise to the MWCNTs/BNC mixture at a rate of one drop per second under constant stirring to incorporate the nanoparticles into the nanocomposite. After this step, the solution was sonicated in an ultrasonic bath for 1 h, and the resulting material was dried in an oven at 60 °C for 4 h. Once dried, a suspension of MWCNTs/BNC-AgNPs was prepared in ultrapure water at a concentration of 1.0 mg mL<sup>-1</sup>.

To synthesize the composite without BNC, 20 mg of functionalized MWCNTs were dispersed in 20 mL of ethanol containing sodium dodecyl sulfate (SDS) at a 10:4 (m/m) MWCNTs:SDS ratio and sonicated in an ultrasonic bath for 30 min. Nanoparticle formation was then carried out using the same conditions described above. Afterward, the mixture was centrifuged for 15 min at 5000 rpm to separate the solid and liquid phases, washed with ethanol, and dried. The resulting MWCNTs-AgNPs material was finally resuspended in ethanol at the same concentration.

### Modification of the GC electrode with MWCNTs/BNC-AgNPs

A carbide sandpaper followed by an aqueous alumina suspension (0.3 μm) was used to polish the surface of the GC electrodes. After polishing, the electrodes underwent a cleaning procedure via cyclic voltammetry in 0.2 mol L<sup>-1</sup> PBS (pH 7.0), consisting of a potential hold at +1.55 V for 45 s, then -1.55 V

for 45 s, followed by 10 cyclic voltammetry scans from -1.55 V to +0.5 V at a scan rate of 100 mV s<sup>-1</sup>. The electrodes were then dried, and 10 µL of the synthesized nanocomposite suspension (1.0 mg mL<sup>-1</sup>) was drop-cast onto each electrode surface. To ensure composite homogeneity, the suspension was sonicated for 5 min prior to application. The modified electrodes were dried at 50 °C and subsequently used in the electrochemical experiments.

### **Electrochemical characterization**

Cyclic voltammetry (CV) and electrochemical impedance spectroscopy (EIS) were used to characterize the electrodes in 5.0 mmol L<sup>-1</sup> [Fe(CN)<sub>6</sub>]<sup>3-/4-</sup> containing 0.1 mol L<sup>-1</sup> KCl. CV scans were recorded from -0.5 to +1.2 V at 100 mV s<sup>-1</sup>. EIS was performed at under open-circuit potential, with a frequency range from 10<sup>7</sup> to 10<sup>-2</sup> Hz and 10 mV amplitude.

Furosemide analysis was carried out in 0.2 mol L<sup>-1</sup> PBS (pH 3.0) using CV (-0.5 to +1.5 V, 50 mV s<sup>-1</sup>) and differential pulse voltammetry (DPV) under optimized conditions: amplitude 100 mV, modulation time 50 ms, step potential 10 mV. The standard addition method was applied for FUR quantification.

### **Preparation and analysis of FUR in synthetic urine**

Furosemide was diluted in ethanol in a concentration of 1 mmol L<sup>-1</sup> in a dark glass and kept away from the light during the analysis. Synthetic urine was prepared following the procedure described by Barreto *et al.* (2024),<sup>21</sup> by dissolving 25.00 g of urea, 1.10 g of CaCl<sub>2</sub>·2H<sub>2</sub>O, 2.92 g of NaCl, 2.25 g of Na<sub>2</sub>SO<sub>4</sub>, 1.40 g of KH<sub>2</sub>PO<sub>4</sub>, 1.60 g of KCl, and 1.00 g of NH<sub>4</sub>Cl in one liter of ultrapure water. The resulting solution had a pH of 7.0. For the analysis of FUR, the electrochemical cell was filled with 1.0 mL of synthetic urine diluted in 19.0 mL of 0.2 mol L<sup>-1</sup> PBS at pH 3.0. A DPV scan was first performed under optimized conditions to ensure the absence of interfering oxidation peaks in the untreated sample. Subsequently, 1.0 and 2.0 µmol L<sup>-1</sup> of FUR were added to the cell, followed by three successive additions of known concentrations to perform the standard addition method.

## **RESULTS AND DISCUSSION**

### **Morphological and electrochemical characterization of nanocomposites**

The morphological and elemental characterization of the synthesized composites was carried out using field-emission scanning electron microscopy (FEG-SEM) coupled with energy-dispersive X-ray spectroscopy (EDS). In addition, nanoparticle size distribution and elemental mapping analyses were performed. The results are presented in Figure 2 (A–K). Images 2A, 2B, and 2C correspond to the MWCNTs-AgNPs material at increasing magnifications (scale bars: 5 µm, 1 µm, and 500 nm, respectively). The images reveal a dense and entangled network of multi-walled carbon nanotubes, with spherical bright structures distributed along the nanotube matrix, which is an indicator of the successful incorporation of silver nanoparticles. The presence of SDS during synthesis likely contributed to the dispersion and stabilization of AgNPs across the MWCNTs framework, as similarly reported in the literature.<sup>22</sup>

Figures 2D and 2E display the MWCNTs/BNC-AgNPs composite, where a more interconnected and uniform nanotube network is observed, in contrast to Figure 2C, in which MWCNTs agglomerates are clearly visible against the dark background, even in the presence of metallic nanoparticles. Although the BNC fibrils are not clearly distinguishable, the morphology suggests effective integration of both BNC and AgNPs within the MWCNTs structure.<sup>9</sup>

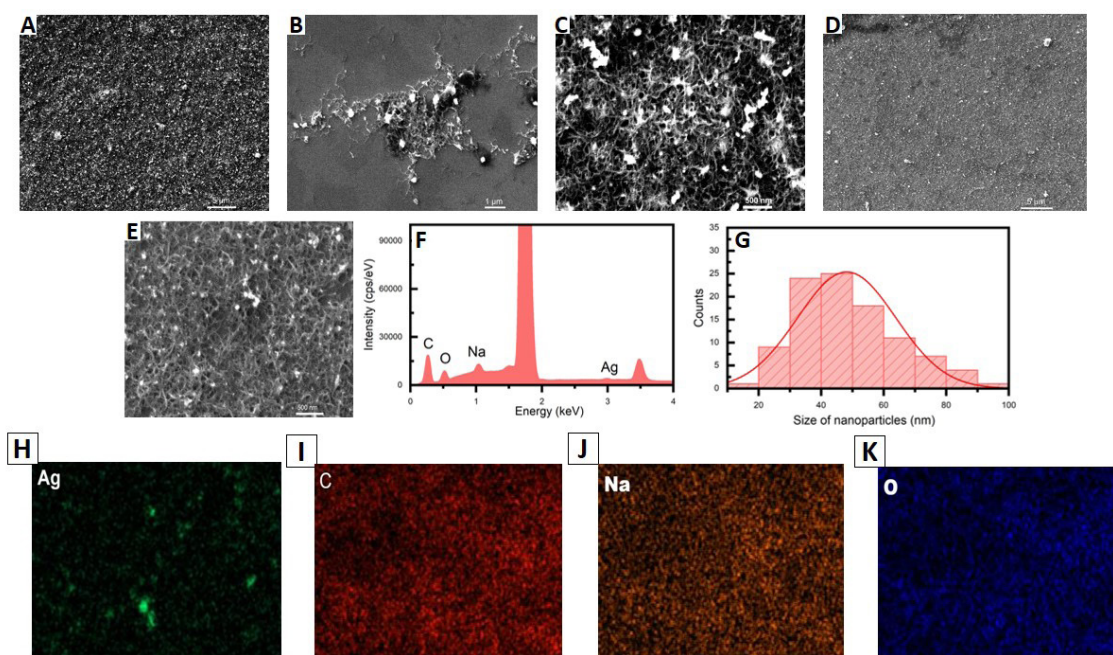


**Figure 2.** FEG-SEM images of (A–C) MWCNTs-AgNPs and (D–E) MWCNTs/BNC-AgNPs nanocomposites. (F) EDS spectrum showing the elemental composition of the MWCNT/BNC-AgNPs composite. (G) Size distribution histogram of AgNPs (18–100 nm). Elemental mapping of (H) Ag, (I) C, (J) Na, and (K) O in the MWCNTs/BNC-AgNPs nanocomposite.

In addition, elemental and size characterization of the silver nanoparticles was performed using energy dispersive X-ray spectroscopy (EDS) and particle size analysis from SEM images. The EDS spectrum (Figure 2F) confirms the presence of carbon (C), oxygen (O), and silver (Ag), indicating successful incorporation of AgNPs into the MWCNTs/BNC composite. The histogram of nanoparticle diameters (Figure 2G) reveals that the AgNPs exhibit size distribution predominantly in the range of 28 to 100 nm, with the most frequent size observed near 55 nm.

Following the morphological and elemental analyses, Figure 2H–K presents the elemental mapping of the MWCNTs/BNC-AgNPs composite. This technique provides a spatial distribution of the main elements on the material's surface. The maps confirm the homogeneous dispersion of carbon (C), oxygen (O), and silver (Ag) throughout the sample. Interestingly, sodium (Na) was also detected. This is likely due to the absence of a washing step in the synthesis protocol, as the use of ultrapure water and lack of visible precipitate after centrifugation led to the assumption that removal was unnecessary. The presence of residual Na highlights the importance of thorough post-synthesis purification steps when high elemental purity is required.

To confirm the effective incorporation of AgNPs on the nanocomposite surface, a comparison was made between an unmodified GC electrode and one modified with MWCNTs/BNC-AgNPs, as shown in Figure S1 in the Supplementary Material. Cyclic voltammetry was performed in the potential range from -0.5 V to +1.5 V at a scan rate of 50  $\text{mV}\cdot\text{s}^{-1}$  to evaluate the redox behavior of silver. A well-defined oxidation peak was observed at +513 mV vs. Ag/AgCl, corresponding to the  $\text{Ag}^0 \rightarrow \text{Ag}^+$  process. A reversible reduction peak appeared at +85 mV, attributed to the  $\text{Ag}^+ \rightarrow \text{Ag}^0$  reaction. These electrochemical features are consistent with previously reported values in literature, confirming the successful deposition and electroactivity of silver nanoparticles on the electrode surface<sup>23,24</sup> and MEV images.<sup>25</sup>

Cyclic voltammetry was employed to evaluate the electrochemical behavior of the electrodes in a redox probe solution consisting of 5.0  $\text{mmol L}^{-1}$   $[\text{Fe}(\text{CN})_6]^{3-/4-}$  and 0.1  $\text{mol L}^{-1}$  KCl prepared in 0.1  $\text{mol L}^{-1}$  PBS (pH 7.0) (Figures S2A and S2B). As summarized in Table I, the GC/MWCNTs/BNC-AgNPs electrode exhibited the most favorable redox response among the evaluated materials. Its anodic peak potential ( $E_{\text{pa}} = 254.06$  mV) shifted to less positive values, indicating enhanced electrocatalytic activity after modification with the

MWCNTs/BNC-AgNPs nanocomposite. Additionally, this electrode displayed the highest peak currents ( $I_{pa} = 97.29 \mu\text{A}$  and  $I_{pc} = -103.27 \mu\text{A}$ ), revealing increased sensitivity and more efficient electron-transfer processes. The peak-to-peak separation ( $\Delta E_p$ ) decreased from 319.82 mV for bare GC to 109.86 mV for GC/MWCNT-AgNPs and further to 95.22 mV for GC/MWCNTs/BNC-AgNPs, confirming the improved charge-transfer kinetics afforded by the nanocomposite.<sup>26</sup>

The enhanced electrochemical response observed for furosemide at the GC/MWCNTs/BNC-AgNPs electrode can be attributed to the synergistic effect of the composite components. MWCNTs provide a conductive network that facilitates electron transfer, while AgNPs act as electrocatalytic sites that promote the oxidation of the analyte. In addition, BNC serves as a porous structural matrix that improves the dispersion of the nanomaterials and increases the accessibility of furosemide to the electroactive surface.

**Table I.** Results obtained from CV experiments of GC, GC/MWCNTs-AgNPs, and GC/MWCNTs/BNC-AgNPs electrodes were recorded in  $5.0 \text{ mmol L}^{-1} [\text{Fe}(\text{CN})_6]^{3-/4-}$  containing  $0.1 \text{ mol L}^{-1} \text{ KCl}$  at a scan rate of  $50 \text{ mV s}^{-1}$  to determine the electrochemical parameters. The analysis considered the anodic ( $E_{pa}$ ) and cathodic ( $E_{pc}$ ) peak potentials, peak-to-peak separation ( $\Delta E_p$ ), anodic ( $I_{pa}$ ) and cathodic ( $I_{pc}$ ) currents, and the  $I_{pa}/I_{pc}$  current ratio.

Electrodes	$E_{pa}$ (mV)	$E_{pc}$ (mV)	$\Delta E_p$ (mV)	$I_{pa}$ ( $\mu\text{A}$ )	$I_{pc}$ ( $\mu\text{A}$ )	$I_{pa}/I_{pc}$
GC	376.43	56.61	319.82	78.95	-81.26	0.93
GC/MWCNT-AgNPs	268.71	161.29	109.86	93.38	-95.37	0.98
GC/MWCNT/BNC-AgNPs	254.06	158.84	95.22	97.29	-103.27	0.94

### Electrochemical behavior of FUR

The electrocatalytic activity of the MWCNTs/BNC-AgNPs nanocomposite toward furosemide oxidation was first investigated by cyclic voltammetry in  $0.2 \text{ mol L}^{-1} \text{ PBS}$  (pH 3.0) within the potential range of  $-0.5$  to  $+1.5 \text{ V vs. Ag/AgCl}$  (Figure 3). The voltammogram showed two irreversible oxidation peaks at approximately  $0.98 \text{ V}$  ( $A_1$ ) and  $1.16 \text{ V}$  ( $A_2$ ) vs. Ag/AgCl. These oxidation processes are attributed to the cleavage of N–R bonds in furosemide, favored by intramolecular hydrogen bonding involving the amine group, which lowers the corresponding bond dissociation energies and facilitates electron transfer.<sup>27</sup> Based on these results, differential pulse voltammetry was subsequently employed to selectively monitor the analyte's oxidation.

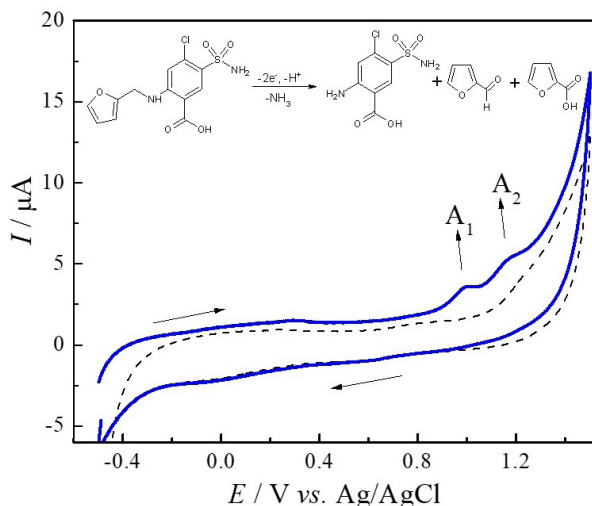


**Figure 3.** CV recorded in a  $0.2 \text{ mol L}^{-1} \text{ PBS}$  (pH 3.0), in the potential range of  $-0.5 \text{ V}$  to  $+1.5 \text{ V}$  in the absence of FUR (dashed line) and in the presence of FUR  $50 \mu\text{mol L}^{-1}$  (solid line) ( $v = 50 \text{ mV s}^{-1}$ ).

The DPV experiments were performed to compare the electrochemical response of the unmodified GC electrode, the GC/MWCNTs-AgNPs electrode, and the electrode additionally incorporating BNC, GC/MWCNTs/BNC-AgNPs. All measurements were carried out in 0.2 mol L<sup>-1</sup> PBS (pH 3.0) using a modulation amplitude of 0.10 V and a step potential of 0.01 V, with the concentration of furosemide fixed at 50 μmol L<sup>-1</sup>. The resulting voltammograms (Figure 4) show a clear improvement in the oxidation signal of FUR upon modification of the electrode surface with conductive and electrocatalytic nanomaterials. The presence of MWCNTs and AgNPs increases the electroactive surface area under the same applied potential, thereby enhancing the redox response of the analyte.<sup>22</sup> Compared with the unmodified GC electrode, the second anodic peak current increased by almost sevenfold, demonstrating the strong catalytic enhancement provided by the nanocomposite.

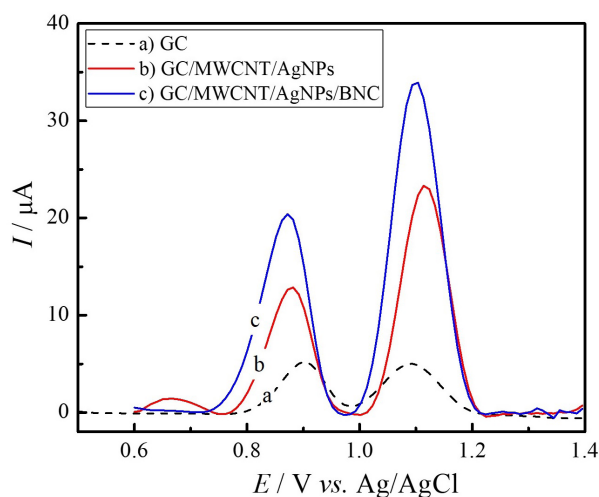


**Figure 4.** Differential pulse voltammograms obtained for (a) GC, (b) GC/MWCNTs-AgNPs, and (c) GC/MWCNTs/BNC-AgNPs in the presence of 50.0 μmol L<sup>-1</sup> furosemide in 0.2 mol L<sup>-1</sup> PBS (pH 3.0). Measurements were recorded in the potential range of 0.6–1.4 V vs. Ag/AgCl. DPV parameters: modulation amplitude = 0.10 V, step potential = 0.01 V, and scan rate = 20 mV s<sup>-1</sup>.

Functionalized MWCNTs contribute by increasing the density of accessible active sites, while AgNPs provide a synergistic effect that accelerates electron-transfer kinetics.<sup>28–30</sup> The incorporation of BNC further improves the nanocomposite by promoting homogeneous dispersion of MWCNTs, increasing charge-transfer efficiency and the number of reactive sites available on the electrode surface.<sup>10,31</sup> Additionally, cellulose can acquire conductive behavior when combined with conductive nanostructures within its matrix.<sup>14</sup> Functionalized MWCNTs also strengthen the composite by enhancing interfacial interactions between the polymeric matrix and the fillers.<sup>10</sup>

Even in the absence of surfactants, ultrasonic treatment assists the uniform dispersion of MWCNTs and nanocellulose in aqueous suspensions.<sup>11</sup> Well-organized CNT networks may exhibit electrical conductivity values up to 50-fold higher than those of entangled structures.<sup>2</sup> Nanocellulose has also proven to be an excellent dispersing agent for MWCNTs,<sup>5</sup> improving their solubilization in water, ensuring better distribution within the matrix, and enhancing both conductivity and structural stability.<sup>32</sup>

The repeatability of the electrochemical response was evaluated by performing 10 consecutive measurements with the same electrode, resulting in relative standard deviation (RSD) values of 2.61% ± 0.59, 2.28% ± 0.31, and 3.79% ± 0.67 for GC1, GC2, and GC3, respectively. The reproducibility was assessed using three independently prepared sensors ( $n = 12$ ), yielding an RSD of 4.43%. These low RSD values demonstrate the good precision and fabrication consistency of the developed sensor.

### Influence of nanocomposite components and DPV settings on analytical response

To enhance the electrochemical response toward FUR, the main experimental variables were systematically optimized. Regarding the nanocomposite composition, different amounts of BNC (2–6 mg) were evaluated, and the best analytical signal was obtained with 2 mg of BNC combined with 20 mg of functionalized MWCNTs. For the synthesis of silver nanoparticles, the amount of silver nitrate varied from 6 to 8 mg, with 8 mg yielding the highest peak current.

The effect of the supporting electrolyte pH was assessed in 0.2 mol L<sup>-1</sup> PBS within the range of pH 3.0 to 8.0, and the most favorable electrochemical performance was observed at pH 3.0. Additionally, key DPV parameters were optimized, with the maximum peak current achieved using a modulation amplitude of 0.10 V and a step potential of 0.01 V. All optimized conditions are summarized in Table II.

**Table II.** Optimized experimental parameters for FUR detection using the GC/MWCNTs/BNC-AgNPs electrode. The effects of BNC and silver nitrate content in the synthesis, PBS (0.2 mol L<sup>-1</sup>) pH, and DPV parameters were evaluated.

Parameters	Optimization Range	Optimized Value
Silver Nitrate in the synthesis (mg)	6-8	8
BNC in the nanocomposite (mg)	2-6	2
pH PBS	3.0-8.0	3.0
Modulation Amplitude	0.01-0.1	0.1
Step	0.001-0.01	0.01

### Calibration curve

A calibration curve was constructed for the target analyte through DPV measurements performed using the optimized experimental conditions. Different concentrations of FUR were analyzed, and the corresponding anodic peak obtained for the second oxidation peak was plotted for each respective concentration, as shown in Figure 5.

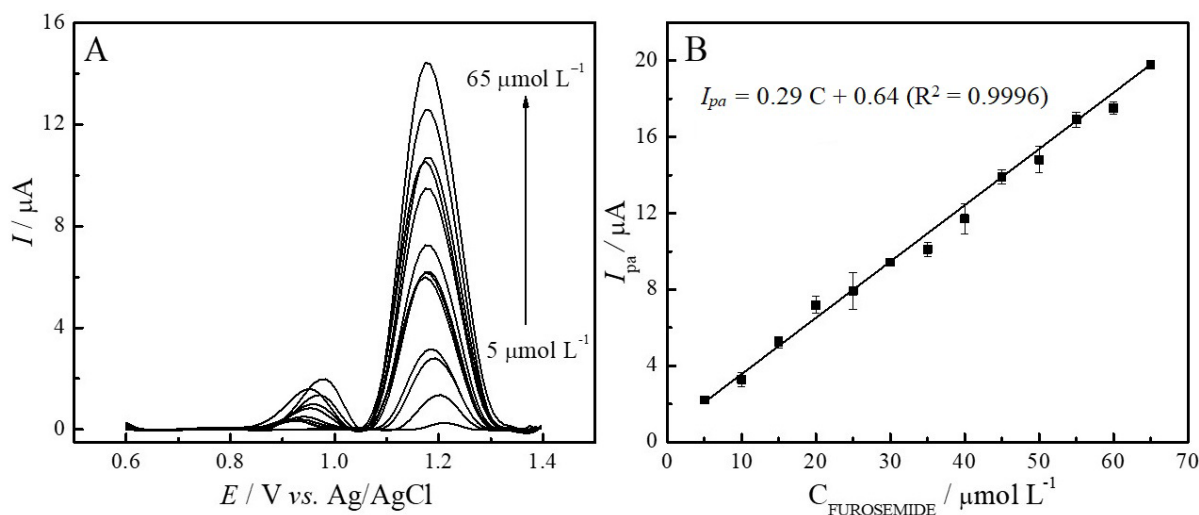


**Figure 5.** (A) DPV voltammograms of FUR in 0.2 mol L<sup>-1</sup> PBS (pH 3.0), with concentrations ranging from 5.0 to 65.0 μmol L<sup>-1</sup>. (B) Calibration curve showing the linear relationship between the anodic peak current ( $I_{pa}$ ) and FUR concentration (DPV conditions: modulation amplitude = 0.1, step potential = 0.01 V, scan rate = 20 mV s<sup>-1</sup>).

The coefficient of determination ( $R^2 = 0.99$ ) indicates a strong linear relationship over the range of 5.0–65.0  $\mu\text{mol L}^{-1}$  for the oxidation peak analyzed, and the equation derived from the curve is presented in Equation 1.

$$I_{pa}(\mu\text{A}) = (0.64 \pm 0.21) + (0.294 \pm 0.003) \times C_{furosemide}(\mu\text{mol L}^{-1}) \quad \text{Equation (1)}$$

The limit of detection (LOD) and limit of quantification (LOQ) were calculated based on standard statistical criteria, using  $3\sigma/b$  and  $10\sigma/b$ , respectively, according to the literature.<sup>27,33</sup> Considering  $\sigma$  as the standard deviation of multiple blank measurements ( $n = 10$ ), and  $b$  the slope of the calibration curve, the LOD and LOQ were calculated, and the values obtained were 0.19  $\mu\text{mol L}^{-1}$  and 0.64  $\mu\text{mol L}^{-1}$ , respectively.

In comparison to existing literature, as shown in Table III, the LOD obtained for the proposal sensor demonstrates competitive analytical performance for furosemide detection. The results highlight the excellent analytical performance of the MWCNTs/BNC-AgNPs nanocomposite, confirming its high sensitivity and reliability. The proposed electrochemical sensor demonstrates sensitivity comparable to HPLC and other conventional sensors, while offering distinct advantages, such as miniaturization, rapid analysis and cost-effective sensor design due to the use of waste-derived nanomaterials and a simplified synthesis with fewer reagents, making it suitable for antidoping detection of furosemide.

Beyond its analytical capability, the main distinction of the proposed platform lies in its rational and sustainable material design. Bacterial nanocellulose derived from beer waste simultaneously acts as a structural matrix and dispersing agent for carbon nanotubes, eliminating the need for conventional surfactants. This multifunctional and water-based fabrication strategy simplifies sensor preparation and represents a more environmentally conscious alternative to previously reported systems.

**Table III.** Comparison of previously reported analytical and electroanalytical methods for FUR determination.

Analytical Method	Supporting electrolyte	Method	LOD ( $\mu\text{M}$ )	Ref
PVC membrane	Borate buffer (pH 9.6)	Potentiometric	119	34
GCE/PEDOT:PSS <sup>a</sup>	PBS (pH 4.0)	DPV	2.0	16
Fe <sub>3</sub> O <sub>4</sub> -GO-SO <sub>3</sub> H-GC <sup>b</sup>	PBS (pH 6.8)	CV	1.5	27
Optical sensor based on hybrid NP	Aqueous medium	FS <sup>e</sup>	0.55	35
MWCNT-paste electrode	BRB <sup>c</sup> (pH 5.0)	CV	0.29	33
HPLC/PAD CFMEs <sup>d</sup>	PBS (pH 7.0)	SWV	0.17	36
GC/carboxyl-MWCNT	BRB <sup>c</sup> (pH 5.7)	DPV	0.0212	18
GC/MWCNTs/BNC-AgNPs	PBS (pH 3.0)	DPV	0.19	This work

<sup>a</sup>Polystyrene Sulfonate-Modified Electrode; <sup>b</sup>Graphene oxide functionalized by chlorosulfonic acid-modified glassy carbon electrode; <sup>c</sup>Britton-Robinson buffer; <sup>d</sup>MWCNT-paraffin oil paste electrode; <sup>e</sup>High pressure liquid chromatography pulsed amperometric detection at cylindrical carbon fiber microelectrodes; <sup>f</sup>fluorescence spectroscopy.

The repeatability and reproducibility of the GC/MWCNTs/BNC-AgNPs electrode were evaluated through continuous DPV measurements at a fixed furosemide concentration of 50.0  $\mu\text{mol L}^{-1}$  in 0.2 mol L<sup>-1</sup> PBS (pH 3.0), using the optimized parameters (modulation amplitude = 0.1 V, step potential = 0.01 V, scan rate = 20 mV·s<sup>-1</sup>).

### Determination of furosemide in synthetic urine

To evaluate the engineered nanocomposite for furosemide doping detection, the MWCNTs/BNC-AgNPs modified electrode was applied in a standard addition and recovery experiment performed in synthetic urine, and FUR was analyzed by DPV at known concentrations. The synthetic urine samples were spiked with 1.00 and 2.00  $\mu\text{mol L}^{-1}$  of FUR in two different experiments, followed by three successive additions of 1.00  $\mu\text{mol L}^{-1}$  to implement the standard addition methodology. The experiments yielded recovery values of 108% and 110%, with relative standard deviations within acceptable limits, demonstrating the potential of this nanocomposite for reliable detection of FUR in real samples.<sup>16</sup>

**Table IV.** Recovery study of FUR in synthetic urine using the proposed electrochemical sensor. Added concentrations, experimentally found values (mean  $\pm$  standard deviation,  $n = 3$ ), and recovery are shown.

FUR added ( $\mu\text{mol L}^{-1}$ )	FUR found ( $\mu\text{mol L}^{-1}$ )	Recovery (%)
1.00	1.08 $\pm$ 0.01	108.00
2.00	2.10 $\pm$ 0.03	110.00

### Influence of interfering agents

The selectivity of the sensor for furosemide detection was evaluated in urine samples, and the influence of potential organic and inorganic interferences was investigated. Real urine comprises a broad range of chemical species. Estriol (a steroid hormone) and copper ions ( $\text{Cu}^{2+}$ ) were selected as model interferences due to their biological relevance and potential to affect analytical responses. The analyses were performed in 0.2 mol  $\text{L}^{-1}$  PBS (pH 3.0) over the potential range of +0.3 to +1.4 V vs. Ag/AgCl, using a fixed concentration of FUR (5.0  $\mu\text{mol L}^{-1}$ ).

Each interferent was added individually in increasing concentrations (2.5, 5.0, and 10.0  $\mu\text{mol L}^{-1}$ ), and the recovery values for FUR were calculated. As shown in Figure 6, the presence of estriol and copper did not significantly affect the electrochemical signal of FUR. These findings confirm the good selectivity of the proposed sensor, particularly when considering the typically low concentrations of such interferences in urine samples. No significant interference from the urine matrix and interferences was observed, indicating good selectivity of the proposed modified electrode for FUR detection.

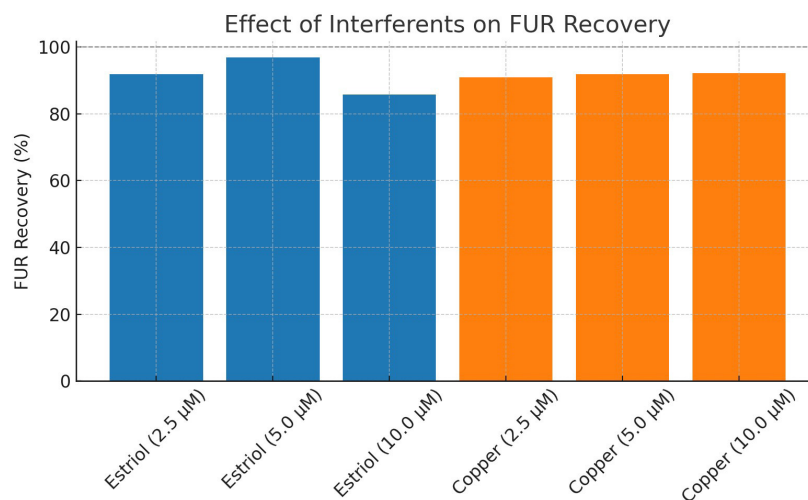


**Figure 6.** Recovery of furosemide (5.0  $\mu\text{mol L}^{-1}$ ) in the presence of estriol and copper at different concentration levels (2.5, 5.0, and 10.0  $\mu\text{mol L}^{-1}$ ), corresponding to molar ratios of 1:2, 1:1, and 2:1 relative to FUR.

## CONCLUSIONS

A new nanocomposite based on multi-walled carbon nanotubes, bacterial nanocellulose obtained from industrial waste, and silver nanoparticles synthesized in ultrapure water without surfactants was successfully developed to modify a glassy carbon electrode for furosemide analysis. Morphological and electrochemical characterizations confirmed the effective incorporation of AgNPs into the MWCNTs network, improving conductivity, catalytic activity, and reducing nanotube agglomeration. After optimization of the DPV parameters, a linear range from 5 to 65  $\mu\text{mol L}^{-1}$  was established for FUR determination, with detection and quantification limits of 0.19  $\mu\text{M}$  and 0.64  $\mu\text{M}$ , respectively. Bacterial nanocellulose exhibited excellent performance as a dispersing and stabilizing agent for MWCNTs,<sup>5</sup> promoting aqueous solubilization, improving matrix homogeneity, and enhancing both conductivity and structural robustness.

## Acknowledgements

The authors thank Coordenação de Aperfeiçoamento de Pessoal de Nível Superior (CAPES) for the research grant and Conselho Nacional de Desenvolvimento Científico e Tecnológico (CNPq) (301516/2022-7).

## Conflicts of interest

The authors declare that they have no known competing financial interests or personal relationships that could have appeared to influence the work reported in this article.

## Use of Artificial Intelligence (AI) tools

The authors acknowledge the use of ChatGPT (OpenAI) and Gemini (Google) for language editing, grammar refinement, stylistic improvements, and assistance with schematic illustrations (Figure 1 and the graphical abstract). All scientific interpretations, experimental design, data analysis, and conclusions were performed and validated by the authors, who take full responsibility for the accuracy, integrity, and originality of the article. No AI tools were used to generate scientific ideas, analyze data independently, or replace the authors' role.

## REFERENCES

- (1) Zaporotskova, I. V.; Boroznina, N. P.; Parkhomenko, Y. N.; Kozhitov, L. V. Carbon Nanotubes: Sensor Properties. A Review. *Mod. Electron. Mater.* **2016**, *2* (4), 95–105. <https://doi.org/10.1016/j.moem.2017.02.002>
- (2) Norizan, M. N.; Moklis, M. H.; Demon, S. Z. N.; Halim, N. A.; Samsuri, A.; Mohamad, I. S.; Knight, V. F.; Abdullah, N. Carbon Nanotubes: Functionalisation and Their Application in Chemical Sensors. *RSC Adv.* **2020**, *10* (71), 43704–43732. <https://doi.org/10.1039/d0ra09438b>
- (3) Ma, P. C.; Siddiqui, N. A.; Marom, G.; Kim, J. K. Dispersion and Functionalization of Carbon Nanotubes for Polymer-Based Nanocomposites: A Review. *Composites, Part A* **2010**, *41* (10), 1345–1367. <https://doi.org/10.1016/j.compositesa.2010.07.003>
- (4) Deng, W.; Zhang, Y.; Wu, M.; Liu, C.; Rahmaninia, M.; Tang, Y.; Li, B. A Tough, Stretchable, Adhesive and Electroconductive Polyacrylamide Hydrogel Sensor Incorporated with Sulfonated Nanocellulose and Carbon Nanotubes. *Int. J. Biol. Macromol.* **2024**, *279* (2), 135165. <https://doi.org/10.1016/j.ijbiomac.2024.135165>
- (5) Miyashiro, D.; Hamano, R.; Umemura, K. A Review of Applications Using Mixed Materials of Cellulose, Nanocellulose and Carbon Nanotubes. *Nanomaterials* **2020**, *10* (2), 186. <https://doi.org/10.3390/nano10020186>
- (6) Durairaj, V.; Liljeström, T.; Wester, N.; Engelhardt, P.; Sainio, S.; Wilson, B. P.; Li, P.; Kontturi, K. S.; Tammelin, T.; Laurila, T.; Koskinen, J. Role of Nanocellulose in Tailoring Electroanalytical Performance of Hybrid Nanocellulose/Multiwalled Carbon Nanotube Electrodes. *Cellulose* **2022**, *29* (17), 9217–9233. <https://doi.org/10.1007/s10570-022-04836-8>

- (7) Rossi, J. E.; Soule, K. J.; Cleveland, E.; Schmucker, S. W.; Cress, C. D.; Cox, N. D.; Merrill, A.; Landi, B. J. Removal of Sodium Dodecyl Sulfate Surfactant from Aqueous Dispersions of Single-Wall Carbon Nanotubes. *J. Colloid Interface Sci.* **2017**, *495*, 140–148. <https://doi.org/10.1016/j.jcis.2017.01.117>
- (8) Trache, D.; Tarchoun, A. F.; Derradji, M.; Hamidon, T. S.; Masruchin, N.; Brosse, N.; Hussin, M. H. Nanocellulose: From Fundamentals to Advanced Applications. *Frontiers in Chemistry* **2020**, *8*, 392. <https://doi.org/10.3389/fchem.2020.00392>
- (9) Durairaj, V.; Liljeström, T.; Wester, N.; Engelhardt, P.; Sainio, S.; Wilson, B. P.; Li, P.; Kontturi, K. S.; Tammelin, T.; Laurila, T.; Koskinen, J. Role of Nanocellulose in Tailoring Electroanalytical Performance of Hybrid Nanocellulose/Multiwalled Carbon Nanotube Electrodes. *Cellulose* **2022**, *29* (17), 9217–9233. <https://doi.org/10.1007/s10570-022-04836-8>
- (10) Durairaj, V.; Li, P.; Liljeström, T.; Wester, N.; Etula, J.; Leppänen, I.; Ge, Y.; Kontturi, K. S.; Tammelin, T.; Laurila, T.; Koskinen, J. Functionalized Nanocellulose/Multiwalled Carbon Nanotube Composites for Electrochemical Applications. *ACS Appl. Nano Mater.* **2021**, *4* (6), 5842–5853. <https://doi.org/10.1021/acsnm.1c00774>
- (11) Taurbekov, A.; Fierro, V.; Kuspanov, Z.; Abdisattar, A.; Atamanova, T.; Kaidar, B.; Mansurov, Z.; Atamanov, M. Nanocellulose and Carbon Nanotube Composites: A Universal Solution for Environmental and Energy Challenges. *J. Environ. Chem. Eng.* **2024**, *12* (5), 113262. <https://doi.org/10.1016/j.jece.2024.113262>
- (12) Urbina, L.; Corcuera, M. Á.; Gabilondo, N.; Eceiza, A.; Retegi, A. A Review of Bacterial Cellulose: Sustainable Production from Agricultural Waste and Applications in Various Fields. *Cellulose* **2021**, *28*, 8229–8253. <https://doi.org/10.1007/s10570-021-04020-4>
- (13) Soheilmoghaddam, M.; Adelnia, H.; Sharifzadeh, G.; Wahit, M. U.; Wong, T. W.; Ali Yussuf, A. Bionanocomposite Regenerated Cellulose/Single-Walled Carbon Nanotube Films Prepared Using Ionic Liquid Solvent. *Cellulose* **2017**, *24* (2), 811–822. <https://doi.org/10.1007/s10570-016-1151-3>
- (14) Jasim, A.; Ullah, M. W.; Shi, Z.; Lin, X.; Yang, G. Fabrication of Bacterial Cellulose/Polyaniline/Single-Walled Carbon Nanotubes Membrane for Potential Application as Biosensor. *Carbohydr. Polym.* **2017**, *163*, 62–69. <https://doi.org/10.1016/j.carbpol.2017.01.056>
- (15) Liu, X.; Xiao, W.; Ma, X.; Huang, L.; Ni, Y.; Chen, L.; Ouyang, X.; Li, J. Conductive Regenerated Cellulose Film and Its Electronic Devices – A Review. *Carbohydr. Polym.* **2020**, *250*, 116969. <https://doi.org/10.1016/j.carbpol.2020.116969>
- (16) Shalauddin, M.; Akhter, S.; Basirun, W. J.; Bagheri, S.; Anuar, N. S.; Johan, M. R. Hybrid Nanocellulose/f-MWCNTs Nanocomposite for the Electrochemical Sensing of Diclofenac Sodium in Pharmaceutical Drugs and Biological Fluids. *Electrochim. Acta* **2019**, *304*, 323–333. <https://doi.org/10.1016/j.electacta.2019.03.003>
- (17) Hossain, M. S.; Khaleque, M. A.; Ali, M. R.; Bacchu, M. S.; Hossain, M. I.; Aly Saad Aly, M.; Khan, M. Z. H. Poly(3,4-Ethylenedioxythiophene): Polystyrene Sulfonate-Modified Electrode for the Detection of Furosemide in Pharmaceutical Products. *ACS Omega* **2023**, *8* (19), 16851–16858. <https://doi.org/10.1021/acsomega.3c00463>
- (18) Wang, Y.; Cheng, J.; Liu, X.; Ding, F.; Zou, P.; Wang, X.; Zhao, Q.; Rao, H. C<sub>3</sub>N<sub>4</sub> Nanosheets/Metal-Organic Framework Wrapped with Molecularly Imprinted Polymer Sensor: Fabrication, Characterization, and Electrochemical Detection of Furosemide. *ACS Sustain. Chem. Eng.* **2018**, *6* (12), 16847–16858. <https://doi.org/10.1021/acssuschemeng.8b04179>
- (19) Heidarimoghaddam, R.; Farmany, A. Rapid Determination of Furosemide in Drug and Blood Plasma of Wrestlers by a Carboxyl-MWCNT sensor. *Mater. Sci. Eng., C* **2016**, *58*, 1242–1245. <https://doi.org/10.1016/j.msec.2015.09.062>
- (20) Abo Zaid, M. H.; El-Enany, N.; Mostafa, A. E.; Hadad, G. M.; Belal, F. Use of Green Fluorescent Nano-Sensors for the Determination of Furosemide in Biological Samples and Pharmaceutical Preparations. *BMC Chem.* **2023**, *17* (1). <https://doi.org/10.1186/s13065-023-00937-y>

- (21) Danesi, E. D. G.; Wosiacki, G. Otimização da produção de nata (celulose bacteriana) por fermentação em superfície. *Cienc. Tecnol. Aliment.* **1998**, *18* (1), 131–139. <https://doi.org/10.1590/s0101-20611998000100027>
- (22) Barreto, F. C.; Mounienguet, N. K.; Ito, E. Y.; He, Q.; Cesarino, I. Coffee Biomass-Based Carbon Material for the Electrochemical Determination of Antidepressant in Synthetic Urine. *Chemosensors* **2024**, *12* (10). <https://doi.org/10.3390/chemosensors12100205>
- (23) Barreto, F. C.; dos Santos, G. T. V.; Leao, A. L.; Goonetilleke, A.; Cesarino, I. Determination and Electro-Remediation of Sulfamethazine Using Carbon Nanotubes and Silver Nanoparticles as Electrode Modifiers. *J. Solid State Electrochem.* **2025**, *29* (3), 1187–1196. <https://doi.org/10.1007/s10008-024-05931-5>
- (24) Donini, C. A.; da Silva, M. K. L.; Simões, R. P.; Cesarino, I. Reduced Graphene Oxide Modified with Silver Nanoparticles for the Electrochemical Detection of Estriol. *J. Electroanal. Chem.* **2018**, *809*, 67–73. <https://doi.org/10.1016/j.jelechem.2017.12.054>
- (25) Barreto, F. C.; Barberis, M. E.; Mounienguet, N. K.; Ito, E. Y.; da Silva, M. K. L.; He, Q.; Cesarino, I. Biosynthesized Silver Nanoparticles Anchored on a Carbon Material Derived from Maple Leaves for the Development of a Green Non-Enzymatic Biosensor for Creatinine Sensing. *Green Analytical Chemistry* **2025**, *13*, 100253. <https://doi.org/10.1016/j.greeac.2025.100253>
- (26) Fekry, A. M.; Abdel-Gawad, S. A.; Tammam, R. H.; Zayed, M. A. An Electrochemical Sensor for Creatinine Based on Carbon Nanotubes/Folic Acid /Silver Nanoparticles Modified Electrode. *Measurement* **2020**, *163*, 107958. <https://doi.org/10.1016/j.measurement.2020.107958>
- (27) Zahran, M.; Khalifa, Z.; Zahran, M. A. H.; Abdel Azzem, M. Recent Advances in Silver Nanoparticle-Based Electrochemical Sensors for Determining Organic Pollutants in Water: A Review. *Mater. Adv.* **2021**, *2*, 7350–7365. <https://doi.org/10.1039/d1ma00769f>
- (28) Hasanzadeh, M.; Pournaghi-Azar, M. H.; Shadjou, N.; Jouyban, A. A New Mechanistic Approach to Elucidate Furosemide Electrooxidation on Magnetic Nanoparticles Loaded on Graphene Oxide Modified Glassy Carbon Electrode. *RSC Adv* **2014**, *4* (13), 6580–6590. <https://doi.org/10.1039/c3ra46973e>
- (29) Qureshi, A.; Shah, A.; Haleem, A.; Shah, I. Electrochemical Detection of Furosemide and Its Removal from Wastewater Using Adsorption Method. *Discover Sustainability* **2025**, *6*, 729. <https://doi.org/10.1007/s43621-025-01663-2>
- (30) Ferrier, D. C.; Honeychurch, K. C. Carbon Nanotube (CNT)-Based Biosensors. *Biosensors* **2021**, *11* (12), 486. <https://doi.org/10.3390/bios11120486>
- (31) Barreto, F. C.; dos Santos, G. T. V.; Barberis, M. E.; Mounienguet, N. K.; da Silva, M. K. L.; He, Q.; Cesarino, I. Renewable Carbon from Flax Shives with Silver Nanoparticles Biosynthesized Using Eichhornia Crassipes Extract for Green Electrochemical Detection of Hydroxychloroquine. *Talanta Open* **2025**, *12*. <https://doi.org/10.1016/j.talo.2025.100548>
- (32) Hosseini, H.; Kokabi, M.; Mousavi, S. M. Conductive Bacterial Cellulose/Multiwall Carbon Nanotubes Nanocomposite Aerogel as a Potentially Flexible Lightweight Strain Sensor. *Carbohydr. Polym.* **2018**, *201*, 228–235. <https://doi.org/10.1016/j.carbpol.2018.08.054>
- (33) Liljeström, T.; Kontturi, K. S.; Durairaj, V.; Wester, N.; Tammelin, T.; Laurila, T.; Koskinen, J. Protein Adsorption and Its Effects on Electroanalytical Performance of Nanocellulose/Carbon Nanotube Composite Electrodes. *Biomacromolecules* **2023**, *24* (8), 3806–3818. <https://doi.org/10.1021/acs.biomac.3c00449>
- (34) Malode, S. J.; Abbar, J. C.; Shetti, N. P.; Nandibewoor, S. T. Voltammetric Oxidation and Determination of Loop Diuretic Furosemide at a Multi-Walled Carbon Nanotubes Paste Electrode. *Electrochim. Acta* **2012**, *60*, 95–101. <https://doi.org/10.1016/j.electacta.2011.11.011>
- (35) Dias, I. L. T.; De Oliveira Neto, G.; Vendramini, D. C.; Sommer, C.; Martins, J. L. S.; Kubota, L. T. A Poly(Vinyl Chloride) Membrane Electrode for the Determination of the Diuretic Furosemide. *Anal. Lett.* **2004**, *37* (1), 35–46. <https://doi.org/10.1081/AL-120027772>

- (36) Saini, A.; Kaur, N.; Singh, N. A Highly Fluorescent Sensor Based on Hybrid Nanoparticles for Selective Determination of Furosemide in Aqueous Medium. *Sens. Actuators, B* **2016**, *228*, 221–230. <https://doi.org/10.1016/j.snb.2016.01.026>
- (37) Guzmán, A.; Agüí, L.; Pedrero, M.; Yáñez-Sedeño, P.; Pingarrón, J. M. Flow Injection and HPLC Determination of Furosemide Using Pulsed Amperometric Detection at Microelectrodes. *J. Pharm. Biomed. Anal.* **2003**, *33* (5), 923–933. [https://doi.org/10.1016/S0731-7085\(03\)00422-9](https://doi.org/10.1016/S0731-7085(03)00422-9)

### SUPPLEMENTARY MATERIAL

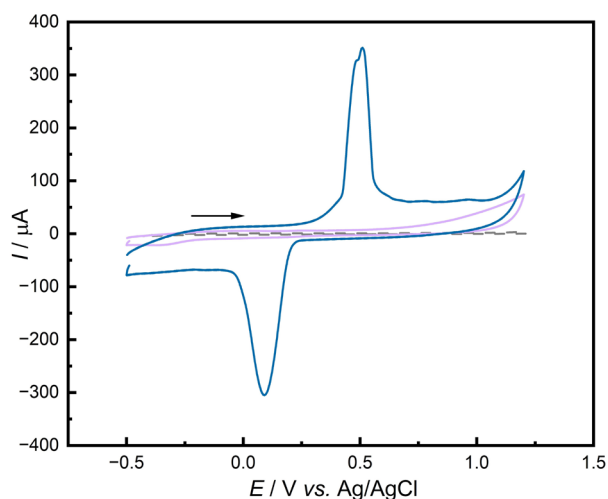


**Figure S1.** CV of GC (dashed black line), GC/MWCNT/BNC (solid purple line), and GC/MWCNT/BNC-AgNPs (solid blue line) recorded in a KCl 0,1 mol L<sup>-1</sup> with  $v = 50 \text{ mV s}^{-1}$  and potential range of  $-0.5 \text{ V}$  to  $+1.2 \text{ V}$ .

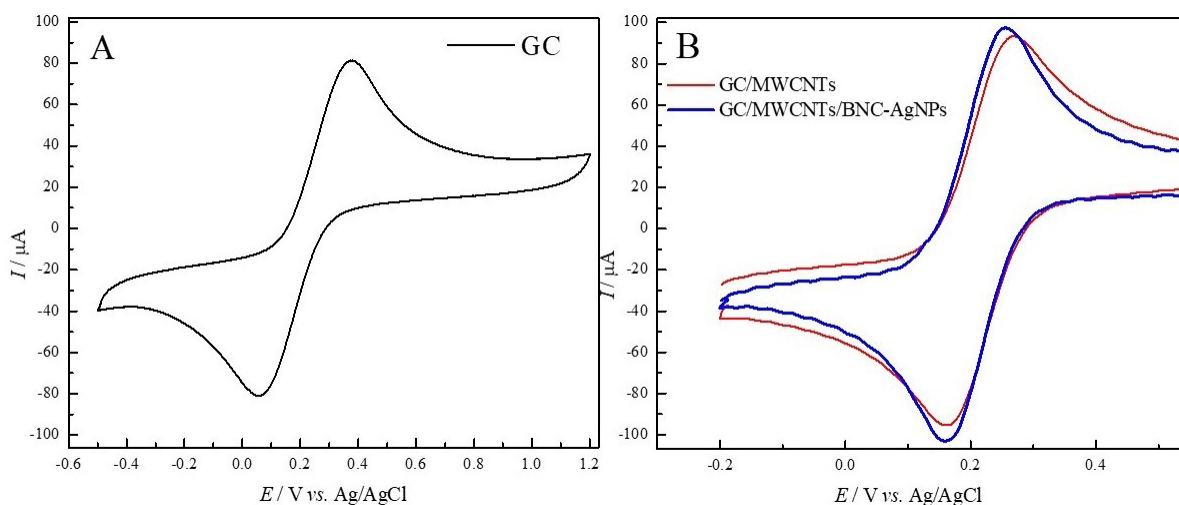


**Figure S2.** Cyclic voltammograms recorded in  $5.0 \text{ mmol L}^{-1} [\text{Fe}(\text{CN})_6]^{3-/4-}$  containing  $0.1 \text{ mol L}^{-1} \text{ KCl}$  in  $0.1 \text{ mol L}^{-1} \text{ PBS}$  ( $\text{pH} = 7$ ) at a scan rate of  $50 \text{ mV s}^{-1}$ . (A) Response of the bare GC electrode. (B) Comparison between GC/MWCNTs and GC/MWCNTs/BNC-AgNPs, showing enhanced redox currents after nanocomposite modification.

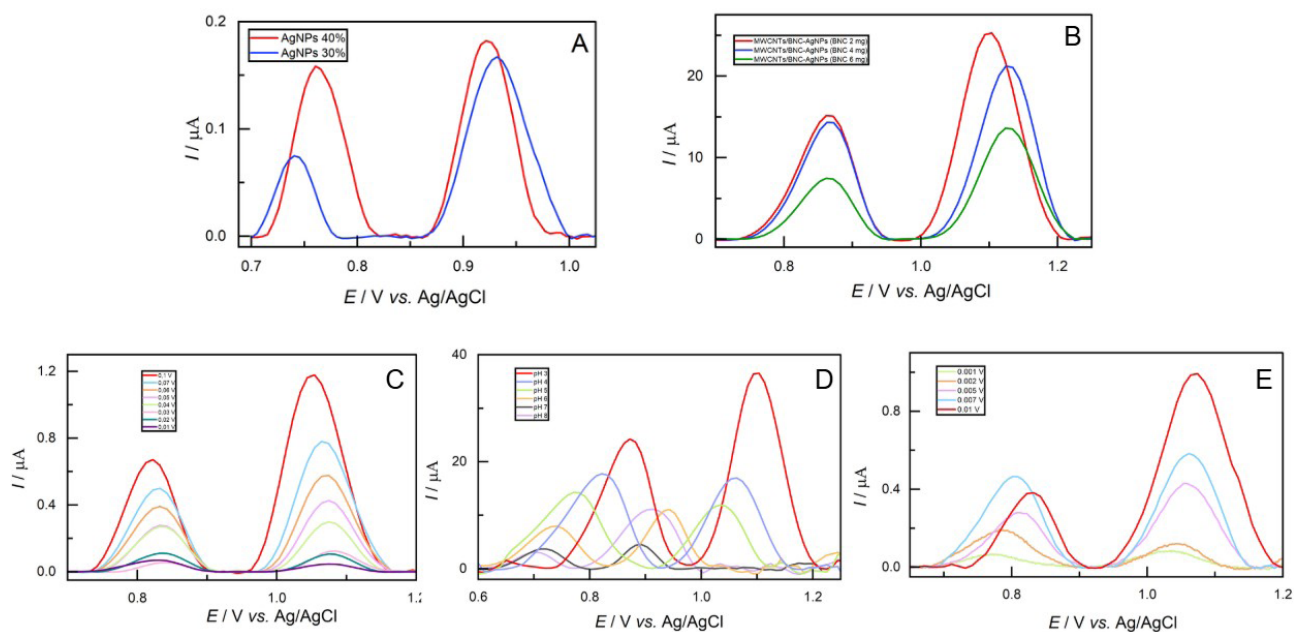


**Figure S3.** Differential pulse voltammograms illustrating the optimization of the experimental parameters listed in Table II: (A) silver nitrate in the synthesis (mg), (B) BNC in the nanocomposite (mg), (C) modulation amplitude, (D) PBS pH, and (E) step potential.